

Thermodynamic State, Temperature Transitions, and Broadband Dielectric Relaxation Behavior in Gradient Interpenetrating Polymer Networks

L. KARABANOVA,¹ P. PISSIS,² A. KANAPITSAS,² E. LUTSYK¹

¹ Institute of Macromolecular Chemistry of National Academy of Sciences of the Ukraine, Kharkov Road 48, Kiev 253660, Ukraine

² National Technical University of Athens, Department of Physics, Zografou Campus, 15780 Athens, Greece

Received 27 February 1997; accepted 14 September 1997

ABSTRACT: Traditional and gradient interpenetrating polymer networks (IPNs) of various composition have been prepared on the basis of crosslinked siliceous polyurethane and a copolymer of butylmethacrylate and dimethacrylate triethylene glycol. For various layers of gradient IPNs cut from the surface to the center of the sample detailed investigations by methods of volume dilatometry, vapor sorption and broadband ac dielectric relaxation spectroscopy were carried out. From data of benzene vapor sorption by various layers of gradient IPN the free energy of mixing of the IPN components has been calculated. For all the layers the free energies of mixing are positive and depend on the distance from the sample surface. Each layer consists of two phases with their own transition temperatures. From these data the composition of each phase for various layers has been calculated. The dipolar α mechanism of the polyurethane-rich phase and the ac conductivity mechanism were studied in detail by analyzing the dielectric susceptibility data within the complex permittivity and the modulus formalism. © 1998 John Wiley & Sons, Inc. *J Appl Polym Sci* 68: 161–171, 1998

Key words: gradient interpenetrating polymer networks; thermodynamic compatibility; free energy of mixing; glass transition; dielectric relaxation spectroscopy

INTRODUCTION

Among the wide variety of polymeric composite materials that have been developed recently, compositions with a gradient of physical or chemical properties have attracted great interest. Gradient interpenetrating polymer networks (IPNs)^{1–3} belong to this class of materials.

Gradient interpenetrating polymer networks are mixtures of crosslinked polymers in which the concentration of one of the networks changes across the section of a sample.⁴ A gradient IPN

may be represented as a combination of an infinite number of layers, each being a full IPN with its own composition and properties. The changing viscoelastic and ultimate properties of such a gradient IPN have been studied and reported elsewhere.⁵ It was shown⁵ that gradient IPNs have a broad maximum of mechanical loss angle tangent spanning a temperature range from 273 to 373 K. The broad maximum is the result of a superposition of a lot of maxima, which characterize the layers with different content of the second network. The elastic modulus of the surface layer and of the center of the gradient sample differ by more than half an order of magnitude in such systems.⁵

It is known⁶ that by chemical crosslinking during IPN formation the phase separation of the

Correspondence to: P. Pissis (ppissis@central.ntua.gr).

Journal of Applied Polymer Science, Vol. 68, 161–171 (1998)
© 1998 John Wiley & Sons, Inc. CCC 0021-8995/98/010161-11

constituent networks takes place due to increased thermodynamic incompatibility. The conditions of phase separation are determined both by the system composition and the reaction kinetics of curing the two networks.

It is evident that for a gradient IPN in each arbitrarily chosen layer the phase separation will proceed to various stages, leading to differences in morphology and properties of each layer. This article deals with detailed investigations of the thermodynamic compatibility, the temperature transitions in various parts (layers), and the dielectric behavior of a gradient IPN based on siliceous polyurethane and a copolymer of butyl methacrylate and dimethacrylate triethylene glycol. The dielectric study can reveal details of the phase structure and provide information about modes of motion in gradient IPNs.^{7,8} Dielectric measurements often reveal more details of the various relaxation processes than the relatively broader features observed in dynamic mechanical spectroscopy and differential scanning calorimetry.^{9,10}

EXPERIMENTAL

Materials

Traditional and gradient IPNs were prepared on the basis of two networks. The first network was crosslinked polyurethane (PUR) and the second network a copolymer of butyl-methacrylate and dimethacrylate triethylene glycol. For preparation of polyurethane three-functional oligoglycol was first synthesized by the reaction of a polyoxypropylene glycol of molecular mass 1052 and phenyl triethoxy silane. The polyurethane elastomer network was then formed from three-functional oligoglycol and adduct of trimethylol propane and toluylene diisocyanate (ratio 1 : 1.5 g-eqv) at temperature 353 K. The IPNs were obtained by sequential curing of components forming the second network. The matrix network (polyurethane) was swelled in monomeric mixture of butyl methacrylate and dimethacrylate triethylene glycol with initiator benzoine isobutyl ether (3.5 wt %), either to the equilibrium state or to any arbitrary degree of swelling to create a concentration gradient. The second network was cured by photopolymerization. By this procedure IPNs with a wide range of composition were obtained.

Gradient IPNs were prepared in the form of blocks 5 mm in thickness. To study the temperature transitions, sorption, and the dielectric pa-

rameters, layers were cut from the surface to the center of the block, each of 0.6 mm thickness. The chemical composition of the IPN and cut layers were determined by chemical analysis for nitrogen.

Vapor Sorption

The benzene vapor sorption of traditional IPNs and of the layers of gradient IPNs were studied using a vacuum installation and a McBain balance. From experimental data on benzene vapor sorption by all the polymer systems we have determined the change in partial free energy of benzene by sorption (dissolution):

$$\Delta\mu_1 = (1/M)RT \ln(P/P_0) \quad (1)$$

where M is the molecular mass of benzene and P/P_0 is the relative vapor pressure. The value $\Delta\mu_1$ changes with solution concentration from 0 to $-\infty$. To calculate the free energy of mixing of the polymer components with solvent we need to know the changes in partial free energy of the polymers (individual networks, IPNs, and the layers).

The difference between the polymer chemical potential in the solution of a given concentration and in pure polymer under the same conditions is $\Delta\mu_2$, which for the polymer components has been calculated according to the Gibbs–Duhem equation:

$$\omega_1 d(\Delta\mu_1)/d\omega_1 + \omega_2 d(\Delta\mu_2)/d\omega_1 = 0 \quad (2)$$

where ω_1 and ω_2 are the weight fractions of solvent and polymer. Hence

$$\int d(\Delta\mu_2) = - \int (\omega_1/\omega_2) d(\Delta\mu_1) \quad (3)$$

By integration over definite limits the values of $\Delta\mu_2$ have been obtained from the experimental data.

The average free energy of mixing of solvent with the individual components, IPNs of various compositions and gradient IPN layers, for solutions of different concentration was estimated according to the equation

$$\Delta g^m = \omega_1 \Delta\mu_1 + \omega_2 \Delta\mu_2 \quad (4)$$

All calculations were performed using a computer program.

Dielectric Relaxation Measurements

Broadband ac dielectric measurements were carried out using three different experimental setups. In the frequency range of 5 Hz to 2×10^9 Hz and the temperature range of 173 to 363 K two Hewlett-Packard Network Analyzers (HP 3755B and HP 8510B) were used. The samples were placed in a shielded capacitorlike measurement cell that was inserted into a transmission line in a homemade thermostatic oven and the transmission coefficient was measured. The dielectric parameters can be determined via these impedance measurements.¹¹ A Schlumberger frequency response analyzer (FRA 1260) supplemented by a buffer amplifier of variable gain was used for measurements in the frequency region 10^{-2} – 10^6 Hz. In the frequency range of 10^2 – 10^7 Hz and the temperature range of 203 to 363 K a Hewlett-Packard HP 4192A Impedance Analyzer was used combined with an Ando type TO-19 thermostatic oven and an Ando SE-70 dielectric cell. We performed complex admittance measurements with a two-terminal electrode configuration. For both setups the samples were clamped between nickel-coated stainless steel electrodes. The samples were in the form of disks of 13 mm diameter and various thickness.

Volume Dilatometry

The temperature transitions of IPNs were studied using volume dilatometry. In this method mercury was used as working liquid in the range of temperatures of 273 to 400 K and polydimethylsilicon as working liquid in the range of 173 to 273 K. The methods of the measurement and of the calculation have already been described.¹²

RESULTS AND DISCUSSION

Figure 1 shows the dependence of nitrogen content (as a measure of the PUR content in the IPN) and of the amount of copolymer on the number of layer in gradient IPN-1 and gradient IPN-2. Layers are numbered from the surface to the center of the samples. The two gradient IPNs differ in the overall amount of copolymer, 36.9% for IPN-1 and 49.6% for IPN-2. It is seen that the mass fraction of copolymer changes from 49% for the first layer to 3% for the third layer in the gradient IPN-1. In the case of gradient IPN-2 the mass fraction of the copolymer changes from 60% for

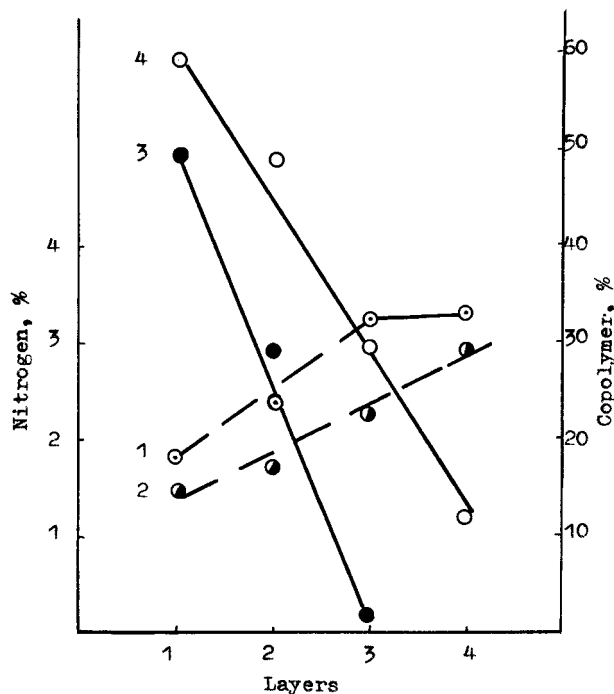


Figure 1 Nitrogen content in layers of gradient IPN-1 (1) and in layers of gradient IPN-2 (2), and copolymer content in layers of gradient IPN-1 (3) and in layers of gradient IPN-2 (4) versus number of layers. Layers are numbered from the surface to the core of the gradient system.

the first (surface) layer to 12% for the fourth (center) layer.

Thermodynamic State of Gradient IPNs

On curing gradient IPNs the conditions for phase separation should be different in different parts of the system due to the composition gradient. It was shown earlier⁶ that the microphase separation in IPNs is incomplete and that the systems have a “frozen” nonequilibrium structure. To estimate the thermodynamic state of gradient IPNs we calculated the free energy of mixing of the constituent networks. For this purpose we have studied the vapor sorption of all the components under investigation. From the experimental data on benzene vapor sorption we calculated the thermodynamic parameters (the method of calculation being described in the Experimental section).

In Figure 2 we show the change of free energy of mixing of benzene with individual PUR, with copolymer and with layers of gradient IPN-1. We can see that all the studied systems (PUR–benzene, copolymer–benzene, gradient layers–benzene)

are thermodynamically stable ($\partial^2 \Delta g^m / \partial \omega_2^2 > 0$). The affinity of benzene for the copolymer (Fig. 2, curve 2) is higher than that for PUR (Fig. 2, curve 1). For layers of gradient IPN-1 the affinity of benzene becomes higher from the first (surface) layer (curve 3) to the third layer (curve 5). (The peculiar behavior of curve 6 (fourth layer, middle of the gradient bulk) is probably explained by a more complex structure, due to meeting there of two diffusion fronts in the course of diffusion of the monomers into the polyurethane matrix network in the process of IPN preparation).

From the concentration dependence of the free energy of mixing of benzene and the system components (Fig. 2), using Hess' law and thermodynamic cycles,¹³ we have calculated the changes in free energy of mixing between the two constituent networks in the various layers of gradient IPN-1. The data are presented in Table I. We can see that the values are positive. Therefore, the compo-

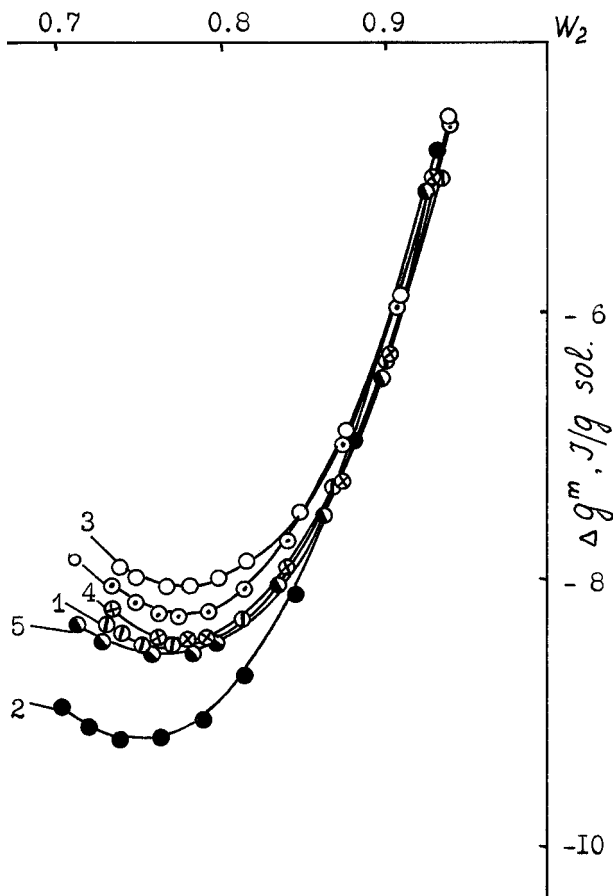


Figure 2 Free energy of mixing Δg^m versus weight fraction of polymer ω_2 of polymer networks with solvent: (1) PUR, (2) copolymer, (3–6) layers of gradient IPN-1.

Table I Variation of the Free Energy of Mixing Δg^x of Siliceous Polyurethane and the Copolymer of Butyl Methacrylate-Triethyleneglycol Dimethacrylate in the Gradient IPN-1 Layers

Layers of Gradient IPN-1	Δg^x (J K ⁻¹ g ⁻¹)
First layer	+1.27
Second layer	+0.45
Third layer	+0.18
Fourth layer	+0.10

nents are incompatible, the whole IPN layer being thermodynamically unstable. The free energy of mixing of the components in the various layers depends on the distance from the sample surface. This effect may be connected not only with the composition variations but also with the changing conditions for phase separation in each layer during IPN formation. The different levels of incompatibility in the different layers influence the structure formed after incomplete phase separation. Each arbitrary layer in the gradient IPN may be considered as an independent two-phase IPN with different composition of constituent phases.²

Temperature Transitions

We have compared the temperature transition data for traditional IPNs of various compositions with the same data for various layers in the gradient IPNs. Figure 3 shows the temperature dependence of the specific volume for traditional IPNs of various compositions. It may be seen that the glass transition temperature for siliceous PUR is 241 K (curve 1), whereas for the copolymer it is equal to 374 K (curve 2). Two transition temperatures were observed for all the IPNs (curves 3–6) corresponding to the presence of two constituent networks, which is typical of a two-phase system. However, in the IPNs all the transition temperatures are shifted in relation to the glass temperature of the individual networks. This shift is the result of incomplete phase separation in the IPNs accompanied by the formation of two phases with varying composition.⁶ The glass temperature (T_g) shift changes regularly with change in IPN composition (Fig. 4). It may be seen that a linear increase in the T_g of the one phase and a linear decrease in T_g of the other phase occurs. A sharp increase in the T_g of copolymer is observed over the composition range 80–100% copolymer in

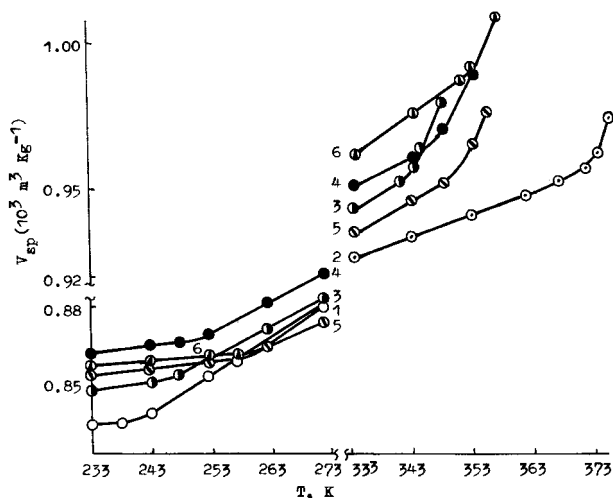


Figure 3 Dependence of specific volume on temperature for traditional IPNs: (1) siliceous PUR; (2) copolymer of butyl methacrylate and dimethacrylate triethylene glycol; (3) IPN with 11 wt % copolymer; (4) IPN with 32 wt % copolymer; (5) IPN with 51 wt % copolymer; (6) IPN with 60 wt % copolymer.

IPNs. This sharp increase may be connected with phase inversion in the system and with a sharp change of the degree of phase segregation.¹⁴

The data obtained when studying transition temperatures of gradient IPN sections, sliced perpendicular to the copolymer concentration gradient, are shown in Figures 5 and 6. The dependence of specific volume on temperature for four sequential sections of gradient IPN-1 (Fig. 5) also shows two temperature transitions, corresponding to the T_g of siliceous PUR copolymer of butyl methacrylate and dimethacrylate triethyleneglycol in the system. There is a regular change in the T_g of the copolymer for the sections from 348 K for the first outer layer, to 343 K for the second layer, to 340 K for the third layer, and to 339 K for the fourth layer. There is also a change in the T_g of siliceous PUR in the layers of gradient IPN-1 from 254 K for the first outer layer to 245 K for the fourth layer.

For gradient IPN-2 (Fig. 6) we observe an analogous situation. The T_g of the copolymer changes from 350 K for the first outer layer to 339 K for the fourth layer. The T_g of siliceous PUR decreases from 261 K for the outer layer to 253 K for the core of gradient bulk.

The comparison of these data with the corresponding data for IPNs of various compositions (Fig. 4) allows the conclusion that the amount of copolymer in the various layers is not the same. Using the data in Fig. 4 as a calibration, the

amount of copolymer in the various layers of gradient IPN-1 and gradient IPN-2 was calculated from their T_g . The amount of copolymer in layers of gradient IPN-1 changes from 40% for the first outer layer, to 18% for the second layer, to 5% for the third layer, and to 2% for the fourth layer. In the gradient IPN-2 the amount of copolymer in the first layer is 51%, in the second 30%, in the third 18%, and in the fourth 5%. These data are in good agreement with those of elemental analysis (Fig. 1), some deviations being ascribed to difficulties in determining the small amount of nitrogen.

On curing gradient IPNs the conditions for phase separation should be different in different parts of the system due to the composition gradient. Since the different polymer mixtures are formed at different distances from the surface of the sample, they differ in morphology and properties.¹⁵ It was shown above (Table I) that the system investigated is thermodynamically unstable. It has positive values of free energy of mixing between the two constituent networks in the various

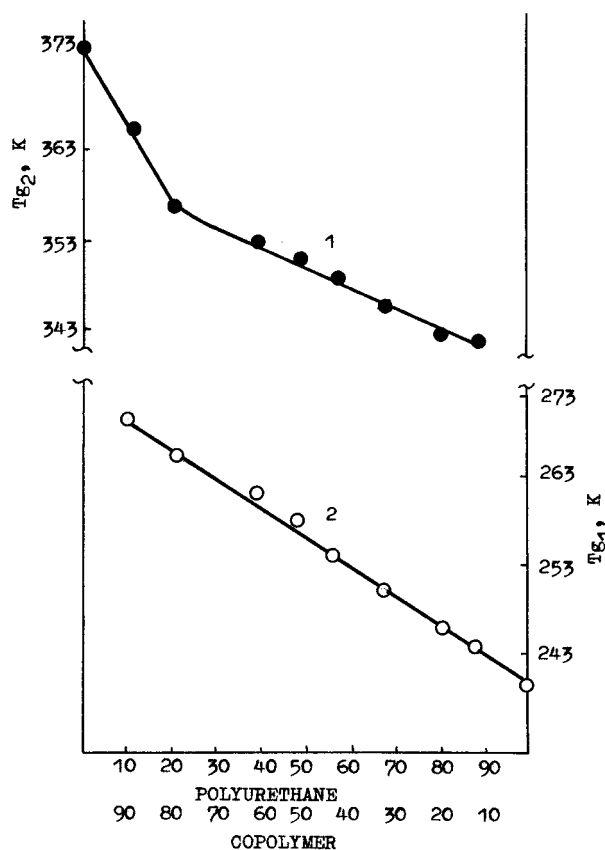


Figure 4 Concentration dependence of glass transition temperature (T_g) for copolymer (1) and for siliceous PUR (2) in traditional IPNs.

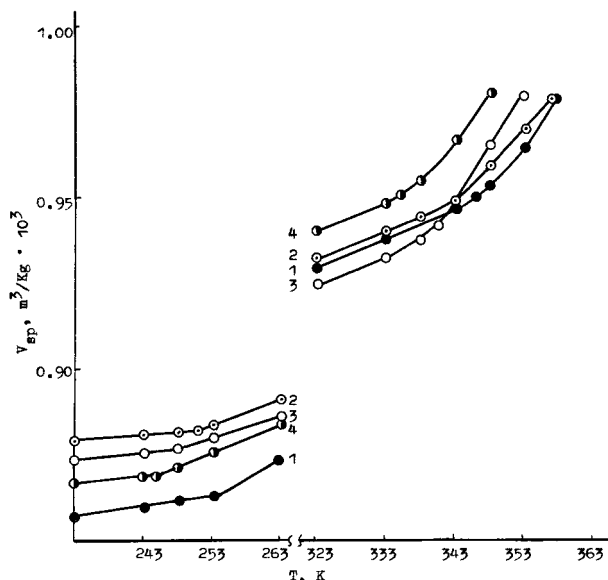


Figure 5 Dependence of specific volume on temperature for layers of gradient IPN-1. Layers are numbered from surface (1) to core (4) of the gradient system.

layers, but the microphase separation in IPNs is incomplete and the systems have a “frozen” non-equilibrium structure. The separation into two phases of different compositions occurs. One phase is the solution of component 1 into the component 2, the second phase is the solution of component 2 into component 1. According to ref. 6, these phases may be considered as an independent quasi-equilibrium IPN. Considering each phase arising in the course of incomplete phase separation as an independent quasi-equilibrium IPN, we can estimate the composition and ratio of these phases. For this purpose we have used the Fox equation,¹⁶ which is valid for compatible polymer blends:

$$1/T_g = \varphi_1/T_{g1} + \varphi_2/T_{g2} \quad (5)$$

where φ_1 and φ_2 are the volume fractions of the components, T_{g1} and T_{g2} are their glass transition temperatures, and T_g is the glass temperature of the compatible blend, which in our case is the glass transition temperature of one of the phases enriched either in PUR or in copolymer. From the corresponding data on the glass temperatures in the IPNs and gradient IPN layers the volume fraction of PU in the PUR-enriched phase was calculated according to the equation

$$\varphi_1 = (T_{g1}T_{g2} - T_gT_g^I)/(T_g^I(T_{g2} - T_{g1})) \quad (6)$$

The volume fraction of copolymer in the copolymer-enriched phase was calculated according to the equation

$$\varphi_2 = (T_{g1}T_{g2} - T_gT_g^{II})/T_g^{II}(T_{g1} - T_{g2}) \quad (7)$$

In these equations T_g^I and T_g^{II} are the transition glass temperatures corresponding to the polyurethane and to the copolymer in the IPN. The data are presented in Table II. The ratio of phases in the various layers was calculated from these data.

From Table II it is seen that changing the ratio of the networks in the traditional IPNs and the layers of gradient IPNs leads to differences in the composition of the evolved phases in the course of formation.

Molecular Mobility in the Gradient IPNs Studied by Dielectric Relaxation Spectroscopy

In Figure 7 we show in log–log plots the dielectric loss $\varepsilon''(f)$ and the loss tangent $\tan \delta(f)$ measured isothermally on layer 1 (outer layer) of gradient IPN-1 in wide ranges of frequency f at temperatures from 253 K up to 363 K. At high frequencies and low temperatures we observe a broad loss peak [more clearly in the $\tan \delta(f)$ plot] which shifts to higher frequencies with increasing temperature. The peak is not present in the pure copolymer network spectra. Its position and the de-

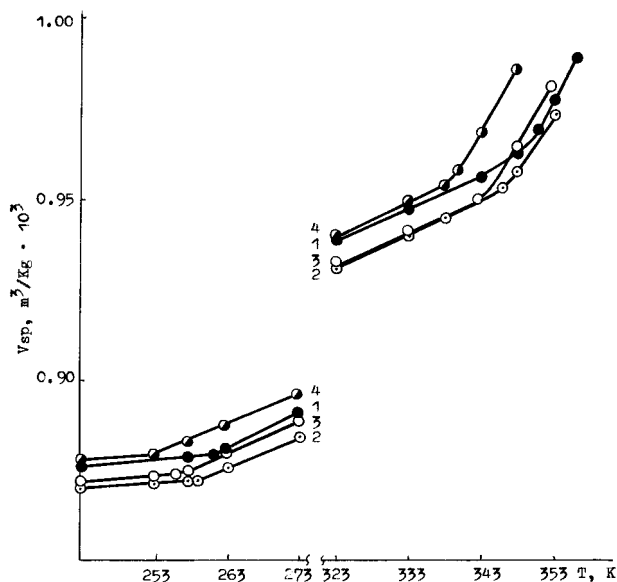


Figure 6 Dependence of specific volume on temperature for layers of gradient IPN-2. Layers are numbered from surface (1) to core (4) of the gradient system.

Table II Glass Transition Temperatures and Phase Characteristics for Traditional IPNs of Various Compositions and of the Layers of Gradient IPNs Based on Siliceous Polyurethane and a Copolymer of Butyl Methacrylate–Triethyleneglycol Dimethacrylate

System	T_{g_1} (PUR) (K)	T_{g_2} (copolymer) (K)	Volume Fraction	
			PUR in PUR Phase (φ_1)	Copolymer in its Phase (φ_2)
Siliceous PU copolymer	241	374		
IPN with 11% of copolymer	245	342	0.9541	0.8305
IPN with 19% of copolymer	247	343	0.9317	0.8362
IPN with 32% of copolymer	251	346	0.8879	0.8533
IPN with 43% of copolymer	255	349	0.8456	0.8702
IPN with 51% of copolymer	259	351	0.8046	0.8813
IPN with 61% of copolymer	262	353	0.7746	0.8922
IPN with 80% of copolymer	266	357	0.7357	0.9137
IPN with 89% of copolymer	270	365	0.6979	0.9553
First layer of gradient IPN-1	254	348	0.8560	0.8646
Second layer of gradient IPN-1	251	343	0.8879	0.8362
Third layer of gradient IPN-1	248	340	0.9206	0.8188
Fourth layer of gradient IPN-1	245	339	0.9541	0.8129
First layer of gradient IPN-2	261	350	0.7845	0.8757
Second layer of gradient IPN-2	259	346	0.8046	0.8533
Third layer of gradient IPN-2	256	343	0.8352	0.8362
Fourth layer of gradient IPN-2	253	339	0.8666	0.8129

pendence of its magnitude on composition allow us to relate it to the main α relaxation associated with the glass–rubber transition of the polyurethane-rich phase ($T_g = 254$ K, Table II). At low frequencies and high temperatures we observe a shoulder in $\varepsilon''(f)$ and $\tan \delta(f)$ spectra (e.g., at 10^3 – 10^4 Hz at 363 K), which we assign to Maxwell–Wagner–Sillars (MWS) interfacial polarization⁸ due to space charges trapped at boundaries between regions of different dc conductivity in the inhomogeneous structure of the IPN. We will study these features in more detail in the next figures. Please note that the temperature at which the MWS shoulder appears (343 K, Fig. 7) is close to the glass transition temperature of the copolymer-rich phase ($T_{g_2} = 348$ K, Table II). This indicates that the MWS peak is related to and probes the increasing mobility of the copolymer-rich phase around its T_g . Finally, the high values of ε'' and $\tan \delta$ (as well as of the real part of permittivity ε' not shown in Fig. 7) at low frequencies and high temperatures indicate the existence of space charge polarization¹⁷ due to the “free” charge motion within the material.¹⁸

Figure 8 shows the relaxation map (Arrhenius plot) for the temperature dependence of the peak frequency of $\tan \delta$ for the primary α relaxation mechanism of PUR and of the polyurethane-rich

phase of the IPNs. As expected for an α mechanism the Vogel–Tamman–Fulcher (VTF) equation⁸

$$f_{\max} = A_{\text{exp}}[-B/(T - T_0)] \quad (8)$$

is a good fit to the data (lines in Fig. 8). The VTF parameters A , B , and T_0 (2×10^{14} s⁻¹, 1338 K and 165 K, respectively for PUR) do not show any systematic variation with sample. We observe in Figure 8 the antiplasticizing action of the copolymer on the α relaxation of PUR: the α relaxation shifts to higher temperatures at fixed frequency and to lower frequencies at fixed temperature in the IPN layers compared to pure PUR, in agreement with the results of specific volume measurements in Figure 5 and Table II. Comparative measurements on PUR and on the IPN layers at the same temperature show that the magnitude of the α relaxation, $\tan \delta_{\max}$, is smaller in the IPNs compared to pure PUR. The $\tan \delta_{\max}$ decreases with the decreasing number of layers from 5 (core) to 1 (surface), reflecting the decreasing amount of PUR with decreasing numbers of layers of the IPN, in agreement with the results of elemental analysis (Fig. 1) and of volume dilatometry. All these results are consistent with the α

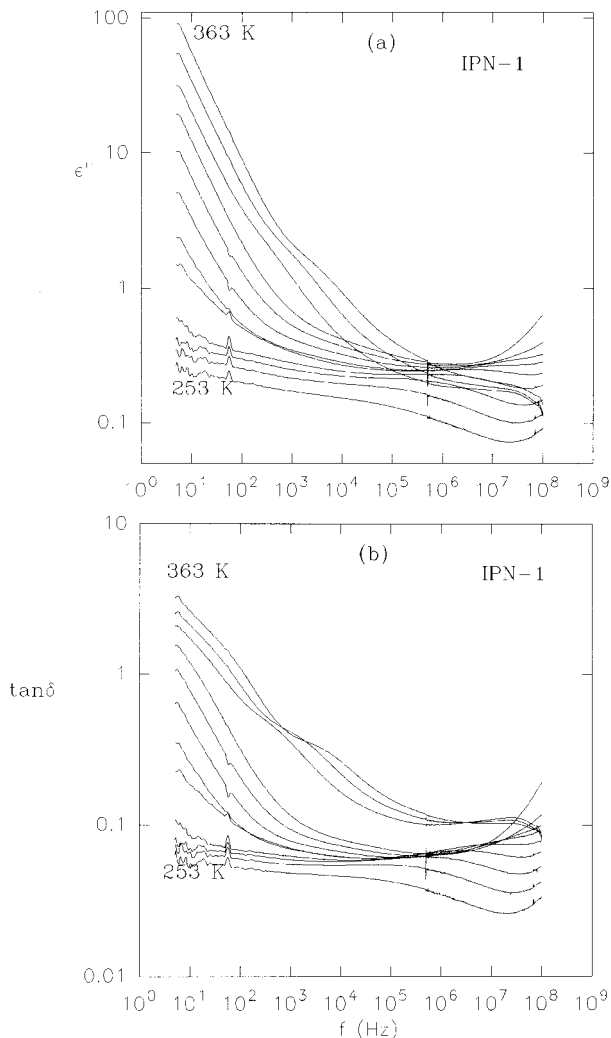


Figure 7 Dielectric loss ϵ'' (a) and loss tangent $\tan \delta$ (b) versus frequency f measured on layer 1 (outer layer) of gradient IPN-1 at several temperatures between 253 and 363 K in steps of 10 K.

relaxation in Figures 7 and 8 being assigned to the PUR-rich phase.

The ac conductivity data in Figure 9 show a tendency toward frequency-independent conductivity at low frequencies (dc conductivity) followed by an increase of conductivity at higher frequencies. At the temperature of measurements in Figure 9 the PUR-rich phase is in the rubbery phase, whereas the copolymer-rich phase is the glassy state (Table II). The main result in Figure 9 is the lower dc conductivity of layer 1 compared to layers 3 and 5 and to pure PUR. In contrast to the α relaxation of the PUR-rich phase in Figures 7 and 8, the dc conductivity reflects properties of the overall morphology, since it is related to the transport of charge carriers over long distances.

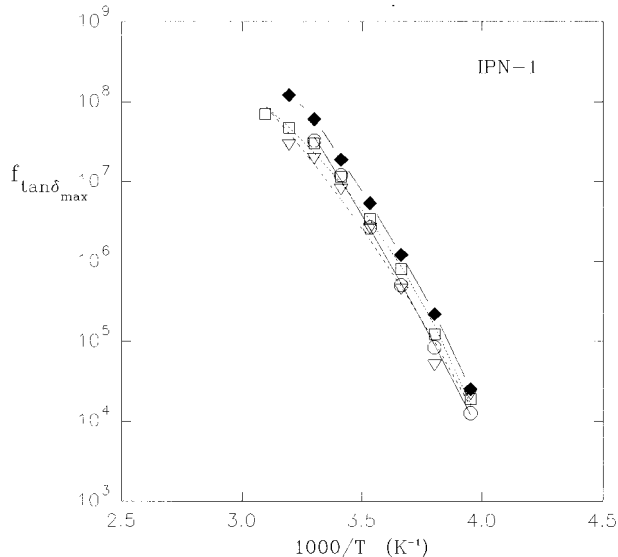


Figure 8 Arrhenius plot of peak frequency of $f_{\tan \delta_{\max}}$ of the α relaxation for PUR (\blacklozenge) and for layer 1 (\circ), layer 3 (∇), layer 5 (\square) of gradient IPN-1. Layers are numbered from surface (1) to core (5) of the gradient system. The lines are fits of VTF equation (8) to the data.

Conductivity effects can be investigated in detail by using the formalism of electric modulus $M^* = 1/\epsilon^*$.^{19–21} Within this formalism, the $M''(f)$ spectra show peaks related to the ionic conductivity and their peak frequencies show the same tem-

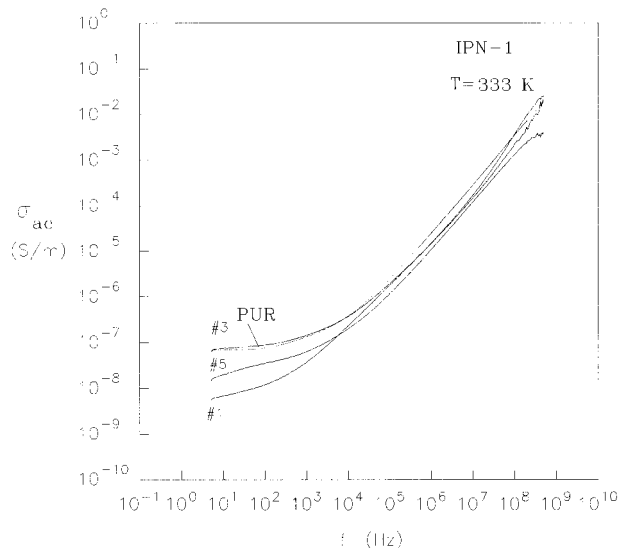


Figure 9 Real part of the ac conductivity σ_{ac} versus frequency f for the PUR network and for layers 1, 3, and 5 of gradient IPN-1. Layers are numbered from surface (1) to core (5) of the gradient system.

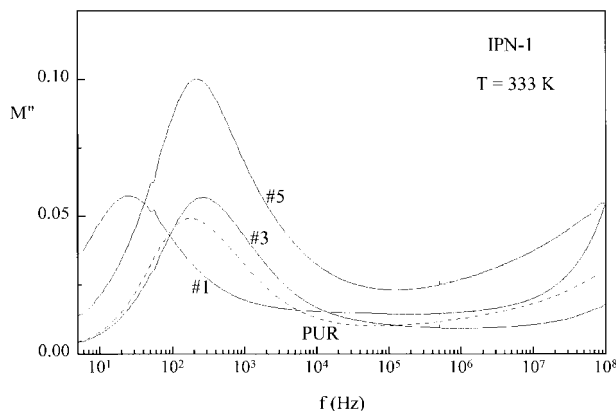


Figure 10 Imaginary part of electric modulus M'' versus frequency f for the pure PUR network and for layers 1, 3, and 5 of gradient IPN-1 at 333 K. Layers are numbered from surface (1) to core (5) of the gradient system.

perature dependence as the dc conductivity.²² Figure 10 shows $M''(f)$ spectra for the samples and the temperature shown in Figure 9. The intense peak at low frequencies, whose frequency position is that of the knee in Figure 9, corresponds to the conductivity relaxation.^{21–23} The frequency of maximum of $M''(f)$ is proportional to the dc conductivity of the sample studied.¹⁹ It follows that the pure PUR network and the IPN-1 layers 3 and 5 show similar dc conductivity to each other and higher than layer 1. As mentioned above this reflects not so much the changes in the composition of the PUR-rich phase (Table II) as properties of the overall morphology and of the amount of copolymer in the layer. It is interesting to note with respect to the results in Figures 9 and 10 that with increasing number of layer from 1 to 5, the T_g of the copolymer-rich phase decreases, approaching the temperature of measurements (333 K), and thus the mobility of the copolymer-rich phase increases. For comparison we show in Figure 11 $M''(f)$ spectra for the pure PUR and the copolymer networks and traditional IPNs. At the temperature of measurements (363 K) only the pure network copolymer is in the glassy state ($T_g = 374$ K, Table II). With increasing copolymer content the $M''(f)$ peak shifts to lower frequencies, that is, the dc conductivity decreases. Please note that the 80% copolymer composition is that around which the phase inversion is indicated to occur (Fig. 4). The peaks we observe at higher frequencies correspond to the dipolar α relaxation of the PUR-rich phase (discussed above) and the β relaxation of the copolymer-rich phase (at 10^4 –

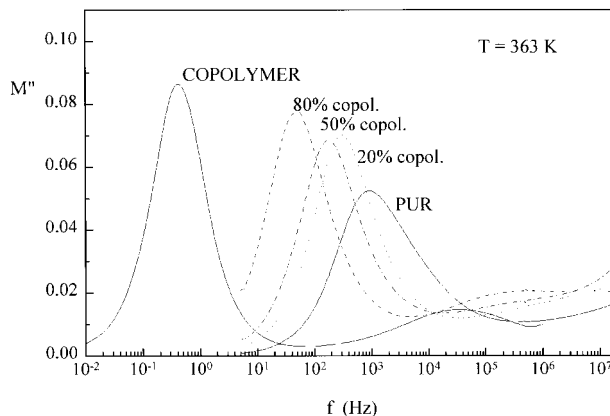


Figure 11 Imaginary part of electric modulus M'' versus frequency f for the PUR and the copolymer networks and traditional IPNs of several compositions indicated in the plot at $T = 363$ K.

10^5 Hz for the pure copolymer network, not discussed here).

The peak frequency of the $M''(f)$ spectra of the pure PUR network and of layers of IPN-1 is plotted against reciprocal temperature in Figure 12. A VTF-type equation of the form of eq. (8) was fitted to the data for the α relaxation. The results confirm those obtained from Figure 8. An Arrhenius-type equation

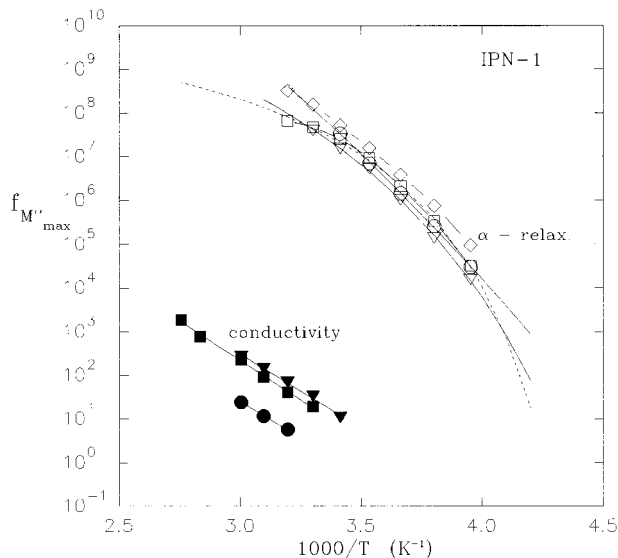


Figure 12 Arrhenius plots of the peak frequency of the $M''(f)$ spectra $f_{M''_{max}}$ for the PUR network (\diamond) and for layer 1 (\circ , \bullet), layer 3 (∇ , \blacktriangledown), layer 5 (\square , \blacksquare) of gradient IPN-1. Layers are numbered from surface (1) to core (4) of the gradient system. The lines are fits of the VTF (α relaxation) and of the Arrhenius equation (conductivity) to the data.

$$f_{M''_{\max}} = f_0 \exp[-E_{\text{act}}/kT] \quad (9)$$

was fitted to the data for the $M''(f)$ peaks at low frequencies (Fig. 10) corresponding to conductivity relaxation in the IPN layers. The conductivity data of the pure PUR (not shown in Fig. 12) network follow a VTF behavior. These results suggest a change of conductivity mechanism in the IPNs compared to pure PUR. In eq. (9) f_0 is the pre-exponential factor, k is Boltzmann's constant, and E_{act} the apparent activation energy of the conductivity relaxation mechanism and, thus, of dc conductivity.²² Table III lists values of E_{act} . They increase with increasing number of layers. Although the changes are small (at the limits of experimental errors), it is interesting to note that E_{act} was found to increase with decreasing content in the traditional IPNs.

In Figure 13 we show the data of Figure 7 in the modulus presentation. Again, at higher frequencies dipolar processes are recorded. Here we focus attention to the low frequency region. With increasing temperature the dc conductivity increases and the $M''(f)$ peak of conductivity current relaxation enters the frequency range of measurements and shifts to higher frequencies. At the three highest temperatures of measurements a second peak appears corresponding to the shoulder in Figure 7. It appears at temperatures close or higher than T_g of the copolymer-rich phase ($T_g = 348$ K, Table II) and is assigned to MWS interfacial polarization, as discussed in details at the beginning of this section. Comparison of Figures 7 and 13 demonstrates the usefulness of different presentation formalisms.

CONCLUSIONS

The thermodynamic behavior, temperature transitions, and dielectric behavior of traditional and gradient interpenetrating polymer networks on the basis of crosslinked siliceous polyurethane

Table III The Apparent Activation Energy of the Conductivity Relaxation Mechanism in the Layers of Gradient IPN-1

Layers of Gradient IPN-1	E_{act} (eV)
1	0.64
3	0.67
5	0.72

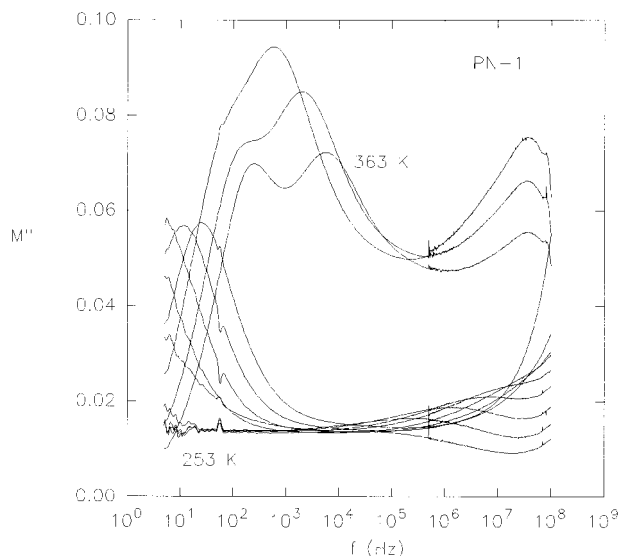


Figure 13 Imaginary part of electric modulus M'' versus frequency f for layer 1 (outer layer) of gradient IPN-1 at several temperatures between 253 and 363 K in steps of 10 K.

and a copolymer of butyl methacrylate and dimethacrylate triethylene glycol have been investigated.

The free energies of mixing of the IPN components in the layers of the gradient systems are positive and depend on the distance from the sample surface. Therefore, the components are incompatible. The different levels of incompatibility in the different layers may be connected not only with the composition variations but also with the changing conditions for phase separation in each layer during IPN formation.

Each layer of the gradient IPNs studied consists of two phases with their own transition temperatures. There is a regular change in T_g of the copolymer and of the polyurethane for the layers from the surface to the center of the gradient system.

The α relaxation loss peak of polyurethane-rich phase in the layers of gradient IPN-1 shifts to lower frequencies compared to that of the pure PUR. Thus, the molecular motions involved in the α relaxation process of PUR become slower in the presence of the copolymer in the layers of the gradient system.

Conductivity effects reflect properties of the overall morphology, as they arise from charge carrier motions over long distances. In the traditional IPNs the conductivity current relaxation mechanism becomes slower (i.e., the dc conductivity decreases) with increasing amounts of copolymer in the IPN. For the gradient IPNs the dc conductiv-

ity increases with increasing distance from the surface of the gradient system.

Thus, the properties of the gradient IPNs are determined not only by the existence of compositional gradient but also by the existence of microphases. The microphases determine the heterogeneity and the different types of morphology and, consequently, the physical properties.

Financial support by INTAS (INTAS 93-3379 and 93-3379-Ext) is gratefully acknowledged. L. Karabanova acknowledges financial support from the NATO Fellowship Programme.

REFERENCES

1. G. Akovali, K. Biliyar, and M. Shen, *J. Appl. Polym. Sci.*, **20**, 2419 (1976).
2. Yu. S. Lipatov, L. V. Karabanova, L. A. Gorbach, E. D. Lutsyk, and L. M. Sergeeva, *Polymer International*, **28**, 99 (1992).
3. Yu. S. Lipatov and L. V. Karabanova, in *Advances in Interpenetrating Polymer Networks*, Vol. 4, Technomic, Lancaster, PA, 1994, p. 191.
4. L. Sperling, *Interpenetrating Polymer Networks and Related Materials*, Plenum Press, New York and London, 1981.
5. Yu. Lipatov, L. Sergeeva, L. Karabanova, V. Rosovitsky, L. Gorbach, and N. Babkina, *Mechanics of Composite Materials*, **6**, 1028 (1988).
6. Yu. Lipatov, *J. Macromol. Sci. Rev. Macromol. Chem. Phys.*, **C30**, 209 (1990).
7. S. B. Dev, A. M. North, and J. C. Reid, in *Dielectric Properties of Polymers*, F. E. Karasz, Ed., Plenum Press, New York, 1972, p. 217.
8. P. Hedvig, *Dielectric Spectroscopy of Polymers*, Adam Hilger, Bristol, 1977, p. 245.
9. C. Mai and G. P. Johari, *J. Polym. Sci., Polym. Phys. Ed.*, **25**, 1903 (1987).
10. A. K. Rizos, G. Fytas, R. J. Ma, C. H. Wang, V. Abetz, and G. C. Meyer, *Macromolecules*, **26**, 1966 (1993).
11. R. Peltster, *IEEE Trans. MTT*, **43**, 1494 (1995).
12. O. V. Anohin and A. E. Faynerman, *The Physical Methods of Investigation of the Polymers*, Kiev, Naukova dumka, 1981, p. 122.
13. A. Tager, *Vysokomol. Soed.*, **19**, 1654 (1977).
14. B. J. Bauer and R. M. Briber, *Advances in Interpenetrating Polymer Networks*, Vol. 4, Technomic, Lancaster, PA, 1994, 123.
15. Yu. S. Lipatov, V. V. Shilov, V. A. Bogdanovich, L. V. Karabanova, and L. M. Sergeeva, *J. Polym. Sci.: Part B: Polymer Physics*, **25**, 43 (1987).
16. T. G. Fox, *Bull. Am. Phys. Soc.*, **2**, 125 (1956).
17. M. W. Wintersgill and J. Fontanella, *Polymer Electrolyte Reviews 2*, G. McCallum and C. Vincent, Eds. Elsevier, London and New York, 1989, p. 43.
18. A. Kyritsis, P. Pissis, and J. Grammatikakis, *J. Polym. Sci., Polym. Phys.*, **33**, 1737 (1995).
19. C. T. Moynihan, R. D. Bressel, and C. A. Angell, *J. Chem. Phys.*, **55**, 4414 (1971).
20. P. B. Macedo, C. T. Moynihan, and R. Bose, *Phys. Chem. Glasses*, **13**, 171 (1972).
21. K. L. Ngai and S. Martin, *Phys. Rev. B*, **40**, 15 (1989).
22. Y. Fu, K. Pathmanathan, and J. R. Stevens, *J. Chem. Phys.*, **94**, 6323 (1991).
23. J. C. Dyre, *J. Non-Cryst. Solids*, **135**, 219 (1991).